A Magnesium-Induced Conformational Transition in the Loop of a DNA Analog of the Yeast tRNA^{Phe} Anticodon Is Dependent on RNA-like Modifications of the Bases of the Stem†

Richard H. Guenther, Charles C. Hardin, Hanna Sierzputowska-Gracz, Vivian Dao, and Paul F. Agris*

Department of Biochemistry, North Carolina State University, Raleigh, North Carolina 27695

Received April 16, 1992; Revised Manuscript Received July 31, 1992

ABSTRACT: Two single-stranded DNA heptadecamers corresponding to the yeast tRNA^{Phe} anticodon stem–loop were synthesized, and the solution structures of the oligonucleotides, d(CCAGACTGAAGATCTGG) and d(CCAGACTGAAGAU-m^{5}C-UGG), were investigated using spectroscopic methods. The second, or modified, base sequence differs from that of DNA by RNA-like modifications at three positions; dT residues were replaced at positions 13 and 15 with dU, and the dC at position 14 with d(m^{5}C), corresponding to positions where these nucleosides occur in tRNA^{Phe}. Both oligonucleotides form intramolecular structures at pH 7 in the absence of Mg^{2+} and undergo monophasic thermal denaturation transitions (T_m = 47 °C). However, in the presence of 10 mM Mg^{2+}, the modified DNA adopted a structure that exhibited a biphasic "melting" transition (T_m values of 23 and 52 °C) whereas the unmodified DNA structure exhibited a monophasic denaturation (T_m = 52 °C). The low-temperature, Mg^{2+}-dependent structural transition of the modified DNA was also detected using circular dichroism (CD) spectroscopy. No such transition was exhibited by the unmodified DNA. This transition, unique to the modified DNA, was dependent on divalent cations and occurred most efficiently with Mg^{2+}; however, Ca^{2+} also stabilized the alternative conformation at low temperature. NMR studies showed that the predominant structure of the modified DNA in sodium phosphate (pH 7) buffer in the absence of Mg^{2+} was a hairpin containing a 7-nucleotide loop and a stem composed of 3 stable base pairs. In the Mg^{2+}-stabilized conformation, the loop became a two-base turn due to the formation of two additional base pairs across the loop. A "bulged" adenosine residue was produced on the 3′-terminal side of the loop. Therefore, we conclude that the Mg^{2+}-induced structural transition exhibited by the modified DNA, but not by the unmodified DNA, occurs because the tRNA^{Phe}-like modifications, d(U-m^{5}C-U), support a site-specific Mg^{2+} binding. Similar Mg^{2+} binding and Mg^{2+}-induced conformational transitions occur in the anticodon stem and loop of tRNA^{Phe}, which has the similarly placed sequence, ψ-m^{5}C-U. However, there are clear differences between the RNA and DNA structures, some of which may be attributable to the lack of other tRNA^{Phe} base modifications and others to the lack of the 2′-OH in the DNA analog.

Transfer RNAs play pivotal roles in the genetic decoding process as primary participants in protein synthesis. They interact with a number of proteins and other RNAs during maturation and translation and have been studied extensively in the context of both structure and function. Despite these efforts, in many cases a detailed understanding of the relationship between the structural features and functional implications has remained elusive. The crystal structures of several tRNAs have been determined at high resolution and exhibit a similar L-shaped framework. These species include yeast tRNA^{Phe} (Holbrook et al., 1978; Saenger, 1984), *Escherichia coli* tRNA$^{Met}_f$ (Woo et al., 1980), and *E. coli* tRNA^{Asp} (Moras et al., 1980). The complex tRNA structure contains many examples of RNA structural motifs that are of general interest including stacked single-stranded regions, non-Watson–Crick base pairs and triples, hairpins, interior loops, and multibranched junctions [for reviews see Delarue and Moras (1989), Wyatt et al. (1989) and Söll (1990)]. Another extensively studied feature is the large number of chemically diverse modified nucleosides (Agris, 1991; Gehrke et al., 1990; Bjork et al., 1987; Agris & Kopper, 1980). More than 60 modified nucleosides have been characterized in tRNAs, and as a class, tRNA molecules contain a much larger proportion of modified residues than any other type of nucleic acid.

The structure and dynamics of a number of purified tRNA species have been studied in solution using NMR methods (Reid, 1981; Hilbers et al., 1983; Kopper et al., 1983; Hyde & Reid, 1985; Smith et al., 1985; Hare et al., 1985 and references therein; Agris et al., 1986; Schmidt et al., 1987). However, due to overlapping resonances in the nonexchangeable proton region, most of the ^{1}H NMR investigations have been limited to the relatively well-resolved imino protons in the 11–15 ppm range and the methyl peaks near 1 ppm. Detailed analysis of nucleic acid structures using NMR is currently limited to oligonucleotides of less than 30 nucleotides. For example, in order to obtain more detailed information about the structure of tRNA^{Phe}, Clore et al. (1984) studied an RNA pentadecamer corresponding to the anticodon stem–loop. Using a less complex system than a complete tRNA, they were able to assign resonances corresponding to imino, amino, aromatic (H2, H6, H8), and ribose H1′ protons which were then used as the basis for nuclear Overhauser effect (NOE) measurements and model-building studies. However, due to several factors including less dispersed chemical shifts for the sugar protons, less efficient synthetic capabilities, the more labile nature of the backbone, and the greater tendency of RNAs to "aggregate", NMR studies with RNAs have

† These studies were supported by NSF Grant DMB8804161 (P.F.A.) and NIH-BRSG Grant RR7071 (C.C.H.). Partial funding was also provided by the North Carolina Agricultural Research Service.

* To whom correspondence should be addressed.

0006-2960/92/0431-11004$03.00/0

lagged behind studies with DNAs. Thus, with a few exceptions [e.g., Hall et al. (1989) and Davis and Poulter (1991)], ^1H NMR studies with tRNA virtually ceased after 1985. While isotope-labeling and multidimensional methods (Kopper et al., 1983; Smith et al., 1985; Schmidt, et al., 1987; Agris & Sierzputowska-Gracz, 1990) offer the promise of extending the current limits to larger structures, it is unlikely that difficulties such as less ^1H resonance dispersion and size-dependent line broadening will be easily overcome for large oligomers.

DNA analogs of RNAs have been used to determine the specific requirements for 2′-hydroxyl groups in the $tRNA^{Phe}$ (Kahn & Roe, 1988; Pequette et al., 1990) and hammerhead ribozyme (Yang et al., 1991) systems. Single-strand-specific nuclease was used to compare the structures of yeast initiator $tRNA^{Met}_f$ and its analog, $tDNA^{Met}_f$ (Pequette et al., 1990). Similar cleavage patterns were obtained, indicating that the 2′-OH groups in tRNA have a limited role in directing the folding of the macromolecule, apparently restricted to constraints on local conformational features and interactions. In fact, it has been shown that synthetic tDNA analogs corresponding to *E. coli* $tRNA^{Phe}$ and $tRNA^{Lys}$ can be aminoacylated by their cognate aminoacyl tRNA synthetases, albeit with a ca. 3- to 4-fold increase in K_m and a ca. 2- to 3-fold decrease in V_{max} (Kahn & Roe, 1988). Given the advantages of using DNA in ^1H NMR studies, DNA analogs may provide information that cannot be obtained with the corresponding RNA. The characteristics of the native tRNA structure that are solely attributable to the molecule being an RNA versus a DNA (i.e., the contribution of 2′-OH) relative to the specific structural contributions that are made by the many modifications to tRNA nucleosides are still in question (Agris & Sierzputowska-Gracz, 1990). In addition, the properties of nucleosides and sequence that contribute to local structure, relative to those that have long-range effects, need to be determined.

An approach, analogous to the study of domains in large proteins, is to consider the tDNA (and tRNA) structures as collections of domains that fold independently at first and are composed of the stem or stem–loop components of the cloverleaf secondary structure. Investigating the structure of these individual domains may provide insights into independent characteristics and stabilities of the substructures within the larger composite structure. The anticodon and acceptor arms are relatively independent domains and are amenable to this approach. In fact, in the case of *E. coli* $tRNA^{Ala}$, it has been shown that a single G·U base pair in the acceptor stem mini helix is the major determinant for recognition by the cognate aminoacyl-tRNA synthetase (Schimmel, 1989).

The present study demonstrates that RNA-like modifications, and not the 2′-OH, are required for a divalent cation-dependent structural transition of a DNA analog to the anticodon stem–loop of $tRNA^{Phe}$ (referred to as "$tDNA^{Phe}_{AC}$").[1] We find that the DNA forms a hairpin structure with an anticodon-containing, 7-nucleotide loop (CT GAAGA). However, in the presence of 10 mM $MgCl_2$ the DNA sequence when modified in a $tRNA^{Phe}$-like manner forms a more stable, compact hairpin conformation with a two-base turn (GA) and an A-bulge on the 3′-terminal side of the stem. This effect resembles the Mg^{2+}-induced change in the anticodon of $tRNA^{Phe}$ that was detected by Y-base fluorescence and other methods (Labuda & Porshke, 1982; Striker et al., 1989). It also implies that a DNA analog can form an inner-sphere Mg^{2+} binding site that is dependent on RNA-like modifications and similar to the Mg^{2+} site found in the $tRNA^{Phe}$ anticodon stem and loop.

MATERIALS AND METHODS

Sample Preparation. The oligonucleotides used in this study were synthesized using standard phosphoramidite chemistry (Sinha et al., 1984). After removal from the solid support and deprotection, the full-length product was separated from failed sequences by HPLC using a Nucleogen DEAE 60-7 column (Werntges, 1985). The oligonucleotide was eluted with a 0–0.7 M LiCl gradient in 20 mM sodium acetate (pH 5.5) containing 40% acetonitrile. Fractions containing the full-length oligonucleotide were pooled and diluted to lower ionic strength and then reloaded on the column. The molecule was then eluted in a minimum volume with high-salt buffer and precipitated with 2-propanol. The pellet was washed with 70% ethanol, lyophilized to remove any residual alcohol, and then resuspended in water.

Absorbance Thermal Denaturation Analysis. Thermal denaturation profiles were obtained using a Gilford Response System spectrophotometer controlled by the associated Response II Thermal Programming software. Profiles were measured in duplicate and corrected for background absorbance due to buffer components. All transitions were reversible as indicated by hysteresis values of <1% obtained upon cooling the samples.

Circular Dichroism Measurements. Circular dichroism spectra were collected using a Jasco J-600 spectropolarimeter interface to an IBM PC microcomputer. The sample temperature was maintained by placing the sample in either a 1- or 0.1-cm path length cylindrical cell surrounded by an external jacket for recirculating water. All CD data were base line corrected for signals due to the cell and buffer. Results were not effected by a 10-fold increase in DNA concentration, indicating a lack of duplex formation.

NMR Methods. NMR data were obtained on a General Electric 500-MHz Omega spectrometer. The temperature was controlled by a SUN 3/160 computer interfaced to the spectrometer and the variable-temperature control unit. Constant-flow cooling was provided by a Microtrol thermostat unit, and the temperature was monitored via a thermocouple implanted in the probe. Partially deuterated sodium 3-(trimethylsilyl)-1-propanesulfonate (TSP) was used as the internal ^1H chemical shift reference. Imino proton spectra were obtained either by presaturating the HDO signal for 2 s prior to applying the 8.2-μs observation pulse or by using the "1–1 hard pulse" solvent suppression method (Hore, 1983; Otting et al., 1987). One-dimensional ^1H spectra were collected in 16K data sets consisting of 512 scans each. One-dimensional nuclear Overhauser effects (NOEs) were measured using the decoupler for preirradiation and a "1–1 hard pulse" sequence for HDO suppression. The data were obtained in the interleaved on and off resonance preirradiation mode. Preirradiation times of 100, 200, and 600 ms were used to monitor for possible spin-diffusion effects on the NOEs. The extent of decoupler power spillover was determined by preirradiating at variable offsets from the peak. Typically, 2048 scans were collected, and the difference free induction decays were processed using a 4-Hz exponential line broadening. All of the NOE data were acquired at 10 °C.

The homonuclear two-dimensional experiments, 2D phase-sensitive COSY and NOESY, were collected with presaturation of the residual HDO peak and with hypercomplex phase

[1] Abbreviations: CD, circular dichroism; $tDNA^{Phe}_{AC}$, the DNA analog corresponding to the anticodon stem–loop of phenylalanyl transfer RNA; WC, Watson–Crick.

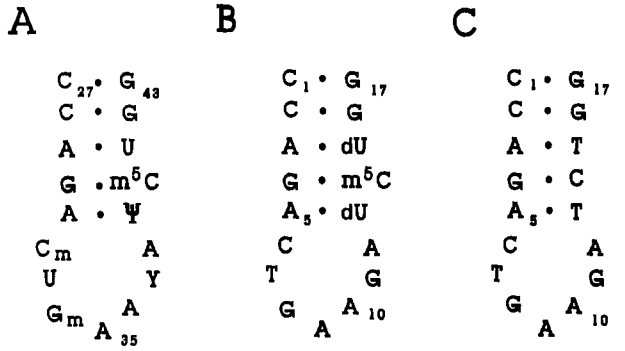

FIGURE 1: Sequence of the yeast $tRNA^{Phe}$ anticodon stem–loop and potential secondary structures formed by the analog $tDNA^{Phe}_{AC}$ sequences. (A) Stem–loop secondary structure formed in the anticodon arm of native yeast $tRNA^{Phe}$. Modified nucleotides include the 2′-*O*-methyl derivatives of C(Cm) and G(Gm), 5-methylcytidine (m^5C), pseudouridine (Ψ), and the hypermodified guanosine derivative wye (Y). The other structures correspond to the monomolecular stem–loops of the (B) modified and (C) unmodified $tDNA^{Phe}_{AC}$ analogs of $tRNA^{Phe}_{AC}$ used in this study. Residues within the modified $tDNA^{Phe}_{AC}$ sequence that were substituted with modified deoxynucleotides in order to better simulate the native $tRNA^{Phe}$ molecule include thymidines 13 and 15 (with dU) and cytidine 14 (with m^5C).

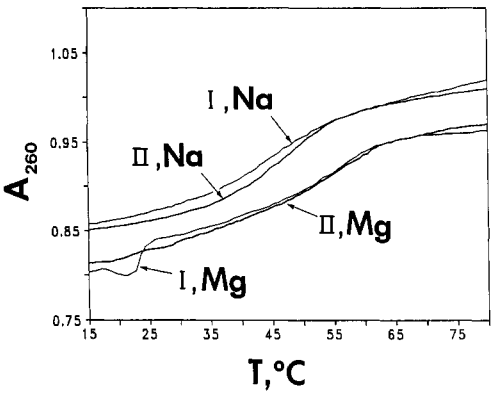

FIGURE 2: Absorbance thermal denaturation profiles obtained with modified and unmodified $tDNA^{Phe}_{AC}$ and monitored at 260 nm. Thermal denaturation was measured in the presence ("Mg") and absence ("Na") of 10 mM $MgCl_2$ in 10 mM sodium phosphate (pH 7) and 0.1 mM EDTA. Results obtained in simultaneous and sequential duplicate analyses demonstrated the reproducible nature of the low-temperature transition observed for modified $tDNA^{Phe}_{AC}$ only in the presence of Mg^{2+} (I, Mg), in comparison to that without Mg^{2+} (I, Na). Unmodified $tDNA^{Phe}_{AC}$ did not exhibit a low-temperature transition in the presence (II, Mg) or absence (II, Na) of Mg^{2+}.

cycling. The data were acquired in 32–128 scans, with a 90° pulse of 7 μs, in 512 blocks, and with 1024 data points per block. The spectral window was 5000 Hz. The data were processed with GE Omega and Felix (Hare, Inc.) software, using a phase-shifted sine bell in the evolution dimension and exponential apodization in the acquisition dimension. The data were zero-filled twice to give a final data set of 1K × 1K. Two-dimensional HOHAHA spectral data were collected with hypercomplex phase cycling, solvent presaturation, and MLEV 17 synchronous decoupler modulation. The data were acquired with a 22-μs 90° pulse on the decoupler channel, which was used for spectral excitation. The spectral window was 4866 Hz. Thirty-two scans were collected in 512 blocks consisting of 1024 data points. The data were processed with a phase-shifted sine bell function in both dimensions and zero-filled to give a final data set of 1K × 1K. No change was seen in the single dimension spectra when the concentration of DNA was reduced by a factor of 10, thereby indicating a lack of hairpin/duplex interconversion.

RESULTS

In order to study the DNA analog of a well-characterized tRNA structure, DNA was synthesized with a base sequence similar to that of the anticodon stem–loop sequence of yeast $tRNA^{Phe}$. Several posttranscriptionally modified nucleotides are present in the native tRNA molecule (Figure 1A). Thus, in order to make one of the tDNA anticodon stem–loop analogs better resemble the native RNA structure, the following modifications were introduced during the synthesis: d(m^5C) at position 14, and dU in place of dT residues 13 and 15 (Figure 1B). This oligonucleotide will be referred to as "modified $tDNA^{Phe}_{AC}$", whereas the unmodified DNA sequence (Figure 1C) is designated $tDNA^{Phe}_{AC}$.

Absorbance Thermal Denaturation Studies. The structure of the tRNA anticodon loop has been shown to change when it forms a complex with Mg^{2+} (Labuda & Porshke, 1982; Striker et al., 1989). Therefore, absorbance thermal denaturation profiles of the structures formed by modified and unmodified $tDNA^{Phe}_{AC}$ were obtained in 10 mM sodium phosphate (pH 7) containing 0.1 mM EDTA and in the absence of $MgCl_2$, or with 5, 10, or 25 mM $MgCl_2$. The results of the thermal denaturation experiments, obtained at a DNA strand concentration of 4.2 μM in 10 mM Mg^{2+}, are shown in Figure 2. Both DNAs exhibited monophasic transitions with a melting temperature (T_m) of 47 °C in the absence of Mg^{2+}. Magnesium increased the T_m of the predominant transition of both DNA structures by 5 °C. However, a second, low-temperature thermal transition at 23 °C was exhibited by the modified $tDNA^{Phe}_{AC}$. The biphasic nature of the transition and T_m values obtained in the presence of Mg^{2+} were not affected by a 10-fold increase in DNA concentration, indicating the events that were being monitored were due to intramolecular interactions. No evidence for duplex formation was obtained.

Circular Dichroism Studies. In order to gain further insight into the structural basis for the low-temperature, Mg^{2+}-dependent transition exhibited by the modified DNA, CD spectra of modified and unmodified DNA were obtained under the same conditions as for the "melt" experiments. Only the CD spectrum of the modified $tDNA^{Phe}_{AC}$ was affected by the addition of Mg^{2+}. The CD band at 268 nm increased, and a more negative ellipticity was observed at 241 nm in the presence of 25 mM Mg^{2+} relative to the modified DNA in buffer alone, which contained 10 mM Na^+. The temperature-dependent spectra in the presence of 25 mM Mg^{2+} are compared to that in the absence of Mg^{2+} in Figure 3, panels B and A, respectively. As the temperature was increased from 10 to 30 °C, the amplitude of the CD maximum at 268 nm for modified $tDNA^{Phe}_{AC}$ with Mg^{2+} decreased to approximately half the initial value (Figure 3B). These results are consistent with the thermal denaturation studies by UV observation that detected a Mg^{2+}-dependent transition occurring in this temperature range. In contrast, without Mg^{2+} only minimal changes were seen in spectra of the modified $tDNA^{Phe}_{AC}$ sample taken over the same temperature range (Figure 3A). As the temperature was increased above the respective T_m values, the spectra taken with and without Mg^{2+} converged to that of a "random coil" species. Similar results were obtained when Mg^{2+} was replaced with Ca^{2+}. However, the changes that occurred in the CD spectrum were only about half as large as seen with Mg^{2+}, indicating that the latter cation induced the transition more effectively. In contrast, no change was obtained when Na^+ was replaced by Li^+, indicating that the effect depends on the divalent charge. The

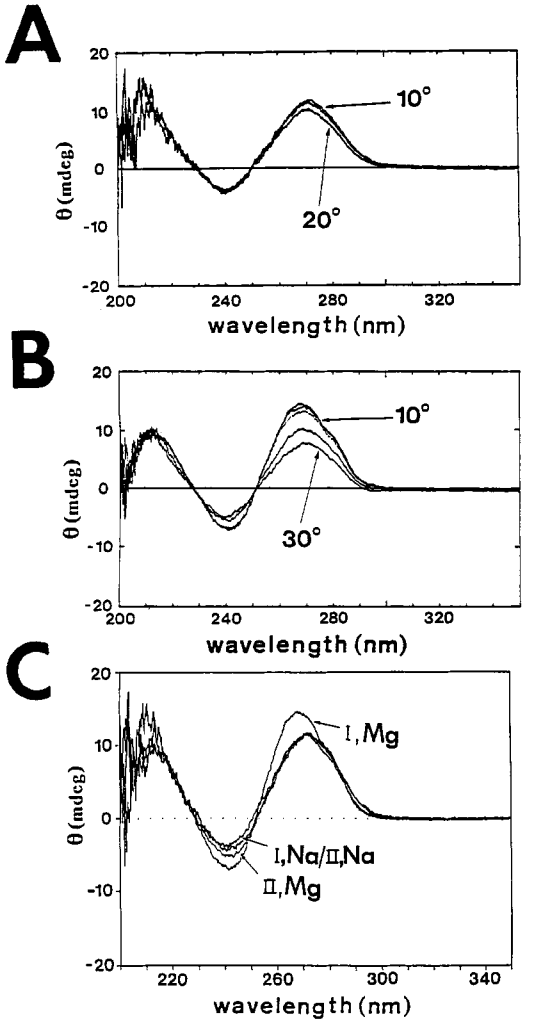

FIGURE 3: Effects of Mg^{2+} on the circular dichroism spectrum of modified and unmodified $tDNA^{Phe}_{AC}$. CD spectra of modified $tDNA^{Phe}_{AC}$ were obtained as a function of temperature in the 10–30 °C range with samples in 10 mM sodium phosphate (pH 7) and 0.1 mM EDTA containing either (A) no added Mg^{2+} or (B) 25 mM $MgCl_2$ in a 1-cm path length cell. Temperatures correspond to 5 °C increments, and the extreme values are labeled. Essentially equivalent results were also obtained at a 10-fold higher DNA concentration in 1-mm path length cells. (C) Differences in ellipticity at ca. 210, 240, 268, and 290 nm in the spectra of modified $tDNA^{Phe}_{AC}$ and unmodified tDNA in the presence and absence of Mg^{2+} at 10 °C. Modified $tDNA^{Phe}_{AC}$ with the added Mg^{2+} (I, Mg) exhibited a CD with a change in wavelength maximum (272–268 nm) and amplitude. Isodichroic points at ca. 220, 242, and 283 nm indicate that Mg^{2+} binds to the oligonucleotide in a two-state process without distinguishable intermediate states. The CD spectra for unmodified tDNA in the presence (II, Mg) and absence of Mg^{2+} (II, Na) were essentially identical to each other and to that of modified tDNA in the absence of Mg^{2+} (I, Na) except for some differences at the 242-nm minima.

addition of Mg^{2+} to modified $tDNA^{Phe}_{AC}$ changed the wavelength maximum of the CD spectrum from 272 to 268 nm and increased the amplitude of the 268-nm band (Figure 3C). In comparison, CD spectra of unmodified $tDNA^{Phe}_{AC}$ in the presence or absence of Mg^{2+} were strikingly similar to each other and to that of the modified $tDNA^{Phe}_{AC}$ in the absence of Mg^{2+} (Figure 3C).

NMR Studies. NMR spectra of modified $tDNA^{Phe}_{AC}$ ($U_{13}m^5C_{14}U_{15}$) in the presence and absence of Mg^{2+} were obtained to determine the structural basis for the observed UV and CD spectral changes that had been induced by Mg^{2+}. In order to detect changes that involved the imino base pairs of the tDNA, ^1H NMR spectra were collected in H_2O with presaturation of the H_2O resonance. In the exchangeable

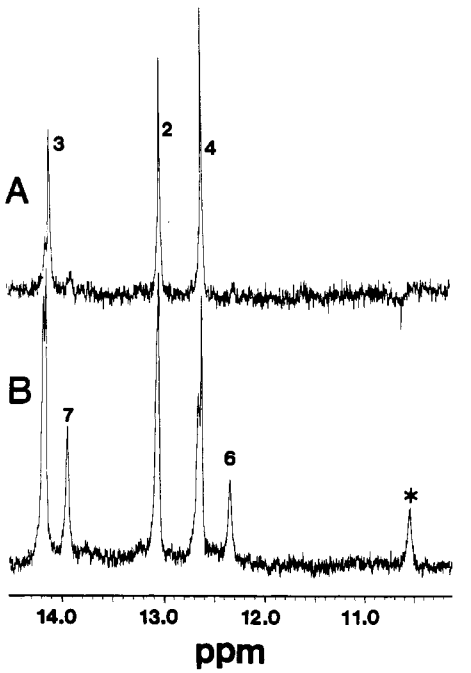

FIGURE 4: Effect of Mg^{2+} on the imino resonances in the ^1H NMR spectrum of modified $tDNA^{Phe}_{AC}$. Spectra were obtained at 10 °C by presaturating the HDO resonance prior to the observation pulse and data acquisition. Spectra were obtained with samples in 10 mM sodium phosphate (pH 7) and 0.1 mM EDTA containing either (A) no added Mg^{2+} or (B) 10 mM $MgCl_2$. Peak labels correspond to imino proton assignments, based on NOE results, and to the numbered base pairs shown in Figure 7. Note that the chemical shifts of the downfield shoulders on the predominant peaks in panel A correspond to the Mg^{2+}-stabilized conformational variant in panel B.

proton region of the spectrum significant spectral changes were observed with the addition of Mg^{2+}. The exchangeable proton region of the NMR spectrum of the modified $tDNA^{Phe}_{AC}$ in 10 mM sodium phosphate (pH 7), 0.1 mM EDTA, and no Mg^{2+} is shown in Figure 4A. The same region of the spectrum after the magnesium concentration is brought to 10 mM is shown in Figure 4B. In the absence of Mg^{2+} the spectrum of modified $tDNA^{Phe}_{AC}$ exhibited three well-resolved imino resonance signals. All three peaks are flanked by small downfield shoulders, suggesting the presence of a minor conformer. Resonances labeled "2" (12.95 ppm) and "4" (12.52 ppm) are in the chemical shift range expected for imino protons in C·G base pairs, and peak 3 (14.05 ppm) is at the position of A·T or A·dU imino protons. Small but clear peaks can also be seen at 13.82 and 12.36 ppm in the absence of Mg^{2+}.

When 10 mM Mg^{2+} was added to the modified $tDNA^{Phe}_{AC}$ sample, resonances 2–4 were still present and the sizes of the resonances at 13.82 and 12.36 ppm (labeled "7" and "6", respectively, in Figure 4B) increased substantially. The resonance labeled "6", at 12.36 ppm, occurs in the spectral region assigned to G·C imino base pairs, and peak 7 is in the A·T region. An additional resonance appeared (labeled "*" at 10.53 ppm) in the chemical shift range of G or T imino protons for guanines that are not involved in Watson–Crick base pairs, but are potentially involved in non-Watson–Crick base interactions (Henderson et al., 1987; Pinnavaia et al., 1975), or for thymines that are "trapped" within T_n hairpin loop structures (Hare & Reid, 1986; Wolk et al., 1988) which do not occur in this DNA sequence. One additional exchangeable proton resonance (Figure 5, labeled "5") is detected both in the presence and in the absence of Mg^{2+} when the spectra were obtained using the "1–1 hard pulse" method instead of presaturation to suppress the water signal.

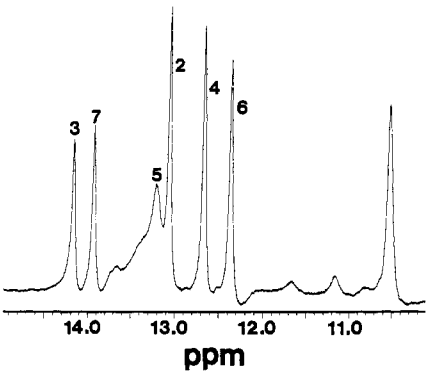

FIGURE 5: Effect of different solvent suppression techniques on the imino proton peak intensities of modified $tDNA^{Phe}_{AC}$ in the presence of Mg^{2+} (10 mM). The spectrum was obtained using the "1–1 hard pulse" method to suppress the HDO resonance. Comparison with the spectrum obtained by presaturating the solvent peak (Figure 4B) demonstrates that the protons are subject to differential exchange (see text).

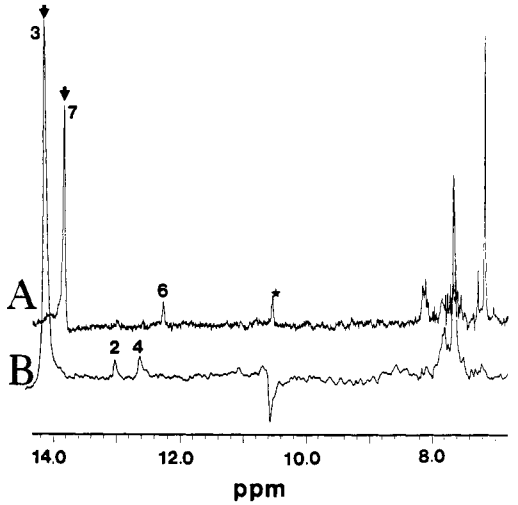

FIGURE 6: Assignment of the imino proton resonances in the ^1H NMR spectrum of the Mg^{2+}-bound form of modified $tDNA^{Phe}_{AC}$. NOE difference spectra showing (A) the connectivity between the T7·A10 imino proton (corresponding to peak 7) and the adjacent C6·G12 imino proton (peak 6) and (B) the connectivities between the A3·dU15 imino proton (peak 3) and those corresponding to the C2·G16 (peak 2) and G4·m^5C14 (peak 4) base pairs.

The imino base pairs were assigned using one-dimensional nuclear Overhauser effect (NOE) spectra (Figure 6), collected in the presence and absence of Mg^{2+}. Assignment of the imino region signals began with the two resonances corresponding to the A·T(dU) base pairs. Only peak 3 had NOEs to both G·C region signals, peaks 2 and 4; peak 3 was assigned to the A·dU base pair in the middle of the modified $tDNA^{Phe}_{AC}$ stem. Signal 2 was the only G·C resonance that had a single NOE to another imino resonance. It was assigned to the second G·C base pair of the stem region, C_2·G_{16}, because the first pair, C_1·G_{17}, although probably transiently intact, was likely to be broadened and lost in the base line due to chemical exchange (fraying). Then, by following the path of all other NOE connectivities, the other imino signal assignments for the stem region were made. The remaining G·C and A·T imino resonances, peaks 6 and 7, had NOE connectivities to each other, but to no other base pairs, and therefore were assigned to $tDNA^{Phe}_{AC}$ loop region base pairs, C_6·G_{11} and T_7·A_{10}. The T_7·A_{10} imino proton signal exhibited an additional NOE to the guanine imino resonance "*", which was then assigned to G_8 in the turn of the loop. It is important to note that 1-D NOEs of peaks 5 and 6 revealed that connectivity

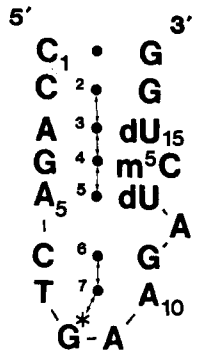

FIGURE 7: Secondary structure of $tDNA^{Phe}_{AC}$ in the presence of 10 mM $MgCl_2$. Proton peak assignments are represented by the numbers in the center of the base pairs; reciprocal NOEs and assigned connectivities are represented by the arrows.

is broken between A_5·dU_{13} and C_6·G_{11}. The interruption of connectivities is due to the internal "bulging" of A_{12} that has base-associated proton NOEs to both G_{11} and U_{13}, indicating a base stacking on the 3′ side of the loop (data not shown). All imino base pair resonance connectivities, and that of the G_8 ("*") imino, that were observed for modified $tDNA^{Phe}_{AC}$ are denoted by arrows in Figure 7. The assignments of nonexchangeable protons were accomplished with 2D COSY, HOHAHA, and NOESY data.

The methyl groups of T_7 and m^5C_{14} in this molecule provided an independent method to confirm the imino signal assignments. For instance, the NOE from the methyl peak of m^5C_{14} to the amino signal at 8.50 ppm is unique to that residue. Preirradiation of imino peak 4 gave a strong NOE to the same amino signal at 8.50 ppm, confirming that peak 4 is correctly assigned. However, the methyl region of the $tDNA^{Phe}_{AC}$ spectrum was composed of four resonances, although only two methyl-containing bases are found in the molecule (Figure 8). The relative sizes and chemical shifts of the four peaks varied with the temperature and magnesium concentration of the sample (Figure 8A,B). The 2-D NOESY (Figure 8C) showed that the four peaks were actually two pairs of signals. The chemical shifts of the methyl resonances that showed connectivity to imino peak 4 were 1.64 and 1.36 ppm, values which are close to those of the m^5C protons in the B and A or Z forms of DNA, respectively (Orbons et al., 1986) and, thus, represent two observed conformations of the $tDNA^{Phe}_{AC}$. The other two methyl peaks, 1.67 and 1.70 ppm, both had connectivities to T_7 located in the loop region of the hairpin. The methyl peaks provided a reasonable measure of the conformational equilibrium under different Mg^{2+} concentrations. With no magnesium present (and at 10 °C), greater than 70% of the oligonucleotide is in the open loop form. At 10 mM Mg^{2+}, greater than 80% of the oligonucleotide is in the closed loop conformation. The same distribution of conformers is seen in other regions of the spectra.

The imino proton exchange rates were different for various parts of the structure in the presence of Mg^{2+}, as well as in its absence. A comparison of the spectrum in Figure 5 with that of Figure 4B demonstrates that peak 5, and, to a lesser extent, peaks 6, 7, and *, had each lost intensity relative to peaks 2–4 when presaturation, rather than the 1–1 pulse method, was used to reduce the water resonance. This indicates that the presaturation energy was transferred relatively efficiently from the solvent to the affected resonances, and one can conclude that the corresponding hydrogen bonds exchanged with the solvent-accessible "open" state more rapidly than those corresponding to the minimally affected peaks. On the basis of results of presaturation experiments,

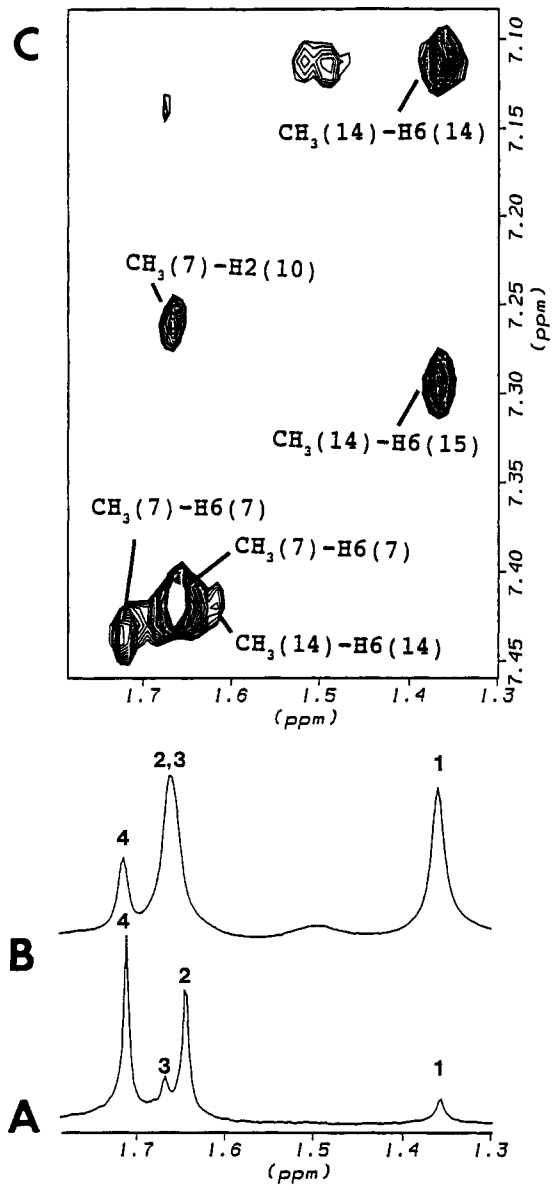

FIGURE 8: Conformational equilibrium of modified $tDNA^{Phe}_{AC}$ effected by Mg^{2+} and revealed in the methyl region of the ^1H NMR spectrum. The methyl region of the one-dimensional ^1H spectra of $tDNA^{Phe}_{AC}$ in the absence (A) and presence (B) of Mg^{2+} exhibits four signals for the two methylated nucleosides in the structure, T_7 and m^5C_{14}. The relative amounts and chemical shifts of the signals change with the addition of Mg^{2+}. The assignment of the signals as two pairs of resonances was aided by their NOE connectivities to base protons as seen in the methyl region of the NOSEY spectum of $tDNA^{Phe}_{AC}$ with Mg^{2+} (C). Methyl signals 1 and 2 are from m^5C_{14}, and signals 3 and 4 are from T_7.

one can qualitatively classify the corresponding imino protons into three classes according to exchange rate: 5 > 6, 7 > 2, 3, 4. Thus, as would be expected, the middle of the stem region is the most stable part of the molecule. The next most stable region is the loop when Mg^{2+} is present. The molecular structure nearest the "bulged A" and at the bottom of the stem (A_5·dU_{13}) is least stable.

To summarize, stem base pairs C_2·G_{16}, A_3·dU_{15}, and G_4·m^5C_{14} are present when Mg^{2+} is not bound to the hairpin. The terminal C_1·G_{17} base pair is probably transiently intact, but not observed. The A_5·dU_{13} base pair is detectable; however, the intensity is reduced, presumably due to an intermediate degree of chemical exchange. In contrast, when Mg^{2+} is bound, in addition to the stem base pairs C_6·G_{11} and T_7·A_{10} also form stable base pairs in the loop region. The A_5·dU_{13} base pair has increased stability, but it is not as stable as the stem or loop base pairs. The imino NOE connectivity pathway is interrupted between A_5·dU_{13} and C_6·G_{11} due to an internal "bulge" formed by A_{12}.

DISCUSSION

The two 17-nucleotide DNA sequences that were synthesized and studied corresponded to DNA analogs of the yeast $tRNA^{Phe}$ anticodon stem and loop with and without RNA-like modifications. On the basis of the optical spectroscopy results presented in this paper, the modified $tDNA^{Phe}_{AC}$ structure is affected by Mg^{2+}, whereas the unmodified tDNA is not. In fact, unmodified $tDNA^{Phe}_{AC}$ exhibited CD spectra in the presence and absence of Mg^{2+} that were identical to each other and to that of modified tDNA in the absence of Mg^{2+}. From the NMR results simple models can be built for the structures of the modified $tDNA^{Phe}_{AC}$ that form in the presence and absence of Mg^{2+}. Temperature-dependent absorbance, "melting", profiles and changes in CD spectra indicated that the Mg^{2+}-bound conformation has more extensive stacking interactions. Increased stacking in the modified tDNA results in a more stable structure in the presence of Mg^{2+} than the one that forms in sodium phosphate (10 mM Na^+, pH 7) buffer alone. The latter is comparable to the structure formed by unmodified tDNA with or without Mg^{2+}. In contrast with studies of other sequences, in which equilibrium mixtures of internal loop containing duplex and hairpin forms were observed (Garcia et al., 1990; Roy et al., 1989; Williamson & Boxer, 1989), no evidence for the presence of a duplex species was found.

NOE studies of the modified $tDNA^{Phe}_{AC}$ in H_2O provided a set of qualitative distance constraints, knowledge of specific hydrogen bonding interactions, and some information about the relative exchange rates of these interactions. The resulting hairpin models are depicted as the stem and seven-membered loop that forms in the absence of Mg^{2+} (Figure 1B), or as the stem and two-base turn that occurs in the presence of Mg^{2+} (Figure 7). The more stable structure, generated in the presence of Mg^{2+}, has a stem with four base pairs (numbered 2–5) on top of two additional and noncontiguous base pairs (numbered 6 and 7) that close the 7-residue loop down to a two-nucleoside turn. The four base pair stem is thought to be separated from the lower two base pairs (C^6·G_{11} and T_7·A_{10}) by a "bulged" A_{12}.

Since the modified $tDNA^{Phe}_{AC}$ structure in Mg^{2+} has two base pairs, C_6·G_{11} and T_7·A_{10}, that do not occur in the anticodon structure of yeast $tRNA^{Phe}$ as deduced by X-ray crystallography (Holbrook et al., 1978) and NMR (Clore et al., 1984), one might prematurely conclude that the former structure is quite different from the latter. However, an examination of the details of the structures does not entirely support this view. The formation of a stem and two-base turn by the modified $tDNA^{Phe}_{AC}$, versus the unmodified tDNA depends specifically on Mg^{2+}. Therefore, one could infer that a particular divalent ion binding site exists in the modified $tDNA^{Phe}_{AC}$ structure, but not that of the unmodified DNA. X-ray crystallography studies demonstrated that an inner-sphere Mg^{2+} coordination complex is formed in the anticodon loop of yeast $tRNA^{Phe}$ (Jack et al., 1977; Quigley et al., 1978). Fluorescence spectroscopy studies showed that the hyper-modified wye (Y) base in the anticodon loop of yeast $tRNA^{Phe}$ can adopt three distinguishable conformations in a Mg^{2+}-dependent manner (Labuda & Porschke, 1982; Striker et al., 1989). These results provide independent evidence for the existence of a specific Mg^{2+} binding site in solution. If one

can extrapolate from the crystallography results to the structure of the modified $tDNA^{Phe}_{AC}$ in solution, one can tentatively place the Mg^{2+}-binding site in the vicinity of C6 and G11, corresponding to Cm32 and Y37 in yeast $tRNA^{Phe}$. These results are entirely consistent with the effects on the imino proton spectrum as assigned on the basis of the NOE data. They would also explain the unusual exchange properties of the imino proton in the A5·dU13 base pair which would be expected to be somewhat perturbed by the bound ion. Therefore, we conclude that the modified DNA analog apparently has ion binding properties that are similar to those of the native tRNA.

How significant is the effect of Mg^{2+} on the structure of modified $tDNA^{Phe}_{AC}$? The ion probably stabilizes the two-base turn of modified tDNA by forming a specific inner-sphere coordination complex and thus neutralizing the repulsive phosphodiester charges. However, the structural details are certainly different from those in the complex found in the anticodon of yeast $tRNA^{Phe}$, in which two of the ligands, Y37 and Ψ39, are modified nucleosides (Quigley et al., 1978). A similar mechanism probably also stabilizes binding of the third strand in RNA pseudoknots (Wyatt et al., 1989, 1990) and triplex DNAs (Pilch et al., 1990; Kohwi & Kohwi-Shigamatsu, 1988). The most important implication is that the ion can modulate the availability of the analog anticodon for potential functional interactions.

How different are the base-paired regions of $tDNA^{Phe}_{AC}$ in solution and yeast $tRNA^{Phe}$ in the crystal? The bases in $tRNA^{Phe}$ 2′-*O*-methyl C_{32}, Y_{37}, U_{33}, and A_{36}, corresponding to C_6·G_{11} and T_7·A_{10} in $tDNA^{Phe}_{AC}$, do not form intraloop base pairs in the $tRNA^{Phe}$ crystal structure. The decoding function of tRNA requires that the anticodon bases be available for base pairing interactions with the mRNA codon. The internally base-paired structure that is adopted by modified $tDNA^{Phe}_{AC}$ in the presence of Mg^{2+} would be incompatible with the coding requirement. Therefore, the propensity for forming a structure with an available anticodon must be either a property that is intrinsic to RNA or due to the presence of the modified nucleotides. We note that Y_{37} of $tRNA^{Phe}$ is unable to form a base pair due to modification of both the imino and amino hydrogen bonding sites. The "bulged" base A_{12} of modified $tDNA^{Phe}_{AC}$ in Mg^{2+} is positioned such that it stacks between G_{11} and U_{13} opposite A_5 and C_6. Thus, the structure of modified $tDNA^{Phe}_{AC}$ mimics the conformation in the vicinity of A_{38} in the $tRNA^{Phe}$ crystal structure. Studies with DNA duplexes that contain bulged A residues indicate that the purine rotates inward and stacks between the other bases in the helix (Woodson & Crothers, 1988 and references therein). Since the U_{33} imino proton of $tRNA^{Phe}$ is hydrogen bonded to the phosphate group of A_{36}, the anticodon loop in the tRNA cannot really be considered a seven-membered loop. Although there are some similarities, particularly a U-m^5C-U sequence-dependent Mg^{2+} binding site and related conformational transition, substantial differences exist between the structures.

Hilbers et al. (1985; Haasnoot et al., 1984) concluded that loops consisting of four or five residues are most stable in DNAs, while RNA hairpins reach a maximal stability with loop sizes of six or seven nucleotides. In contrast with this conclusion, NMR studies have shown that RNA hairpins and internal loops in solution are smaller than expected, forming compact domains that can contain noncanonical conformational features (e.g., synG, C2′-endo sugar pucker), non-Watson–Crick base pairs (e.g., G·U, A·G, A·C), and phosphate–base or 2′-OH–base bonding interactions (Puglisi et al., 1990; Varani et al., 1989, 1991; Heus & Pardi, 1991). Loops in DNAs can also form structures that contain less than four unpaired residues [e.g., Orbons et al. (1987) and Blommers et al. (1991)], and even loops that have been regarded as open are relatively closely knit domains (e.g., T_n loops; Hare & Reid, 1986). It is clear that both types of nucleic acid can readjust to a surprising extent by adopting nonconventional structures in order to minimize the free energy.

The role of modified and hypermodified nucleotides in tRNAs, other RNAs, and DNA has been studied extensively, yet our understanding of their biological purposes and structural mechanisms of action is still quite limited. The importance of d(m^5C) to local structure in the formation of Z-DNA, and in the inhibition of the sequence-specific restriction endonucleases, is well documented. The ability of d(m^5C) to function in the negative regulation of transcription, even when located many base pairs upstream of the transcription start site, is also well recognized. The studies reported here demonstrate that tRNA-like modifications of a DNA analog of yeast $tRNA^{Phe}_{AC}$, including the methylation of cytidine, contribute to the ability of that molecule, and perhaps of the tRNA itself, to site-specifically bind Mg^{2+}, which results in an altered and more stable structure at a location that is structurally distant from the modifications. In the following paper (Dao et al., 1992) we show that the methylated cytosine in the anticodon stem is the single required modified nucleoside for a strong Mg^{2+} binding site and subsequent long-range, conformational transition within the loop.

ACKNOWLEDGMENT

We thank Keith Everett, North Carolina State University Molecular Biology Center, for the synthesis of NMR quantities of the oligonucleotide, Ling Xia for his help in the purification of the oligonucleotide, and Pat Sullivan for her assistance in the preparation of the manuscript.

REFERENCES

Agris. P. F. (1991) *Biochimie* (in press).

Agris, P. F., & Kopper, R. A. (1980) *The Modified Nucleosides of Transfer RNA II*, Alan R. Liss, New York.

Agris, P. F., & Sierzputowska-Gracz, H. (1990) in *Chromatography and Modification of Nucleosides: Part A* (Gehrke, C. W., & Kuo, K. C., Eds.) pp 225–253, Elsevier, New York.

Agris, P. F., Sierzputowska-Gracz, H., & Smith, C. (1986) *Biochemistry 25*, 5126–5131.

Bjork, G. R., Ericson, J. U., Gustaffson, G. A. D., Hagervall, T. G., Jonsson, Y. H., & Wilkstrom, P. M. (1987) *Annu. Rev. Biochem. 56*, 263–287.

Blommers, M. J. J., Van de Ven, F. J. M., Van der Marcel, G. A., Van Boom, J. H., & Hilbers, C. W. (1991) *Eur. J. Biochem. 201*, 33–51.

Clore, G. M., Gronenborn, A. M., Piper, E., McLaughlin, L. H., Graeser, E., & van Boom, J. H. (1984) *Biochem. J. 221*, 737–751.

Dao, V., Guenther, R. H., & Agris, P. F. (1992) *Biochemistry* (following paper in this issue).

Davis, D. R., & Poulter, C. D. (1991) *Biochemistry 30*, 4223–4231.

Delarue, M., & Moras, D. (1989) *Nucleic Acids and Molecular Biology* (Eckstein, F., & Lilley, D. M. J., Eds.) Vol. 3, pp 182–196, Springer-Verlag, New York.

Garcia, A. E., Gupta, G., Soumpasis, D. M., & Tung, C. S. (1990) *J. Biomol. Struct. Dyn. 8*, 173–186.

Gehrke, C. W., Desgres, J. A., Gerhardt, K. O., Agris, P. F., Keith, G., Sierzputowska-Gracz, H., Tempesta, M. S., & Kuo, K. C. (1990) in *Chromatography and Modification of*

Nucleosides: *Part A* (Gehrke, C. W., & Kuo, K. C., Eds.) pp 159–223, Elsevier, New York.
Haasnoot, C. A. G., Westerink, H. P., van der Marel, G. A., & van Boom, J. H. (1984) *J. Biomol. Struct. Dyn. 2*, 345–360.
Hall, K. B., Sampson, J. R., Uhlenbeck, O. C., & Redfield, A. G. (1989) *Biochemistry 28*, 5794–5801.
Hare, D. R., & Reid, B. R. (1986) *Biochemistry 25*, 5341–5350.
Hare, D. R., Ribeiro, N. S., Wemmer, D. E., & Reid, B. R. (1985) *Biochemistry 24*, 4300–4306.
Henderson, E., Hardin, C. C., Wolk, S. K., Tinoco, I., Jr., & Blackburn, E. H. (1987) *Cell 51*, 899–908.
Heus, H. A., & Pardi, A. (1991) *Science 253*, 191–193.
Hilbers, C. W., Heerschap, A., Haasnoot, C. A. G., & Walters, J. A. L. I. (1983) *J. Biol. Struct. Dyn. 1*, 183–207.
Hilbers, C. W., Haasnoot, C. A. G., de Bruin, S. H., Joordens, J. J. M., van der Marel, G. A., & van Boom, J. H. (1985) *Biochimie 67*, 685–695.
Holbrook, S. R., Sussman, J. L., Warrant, R. W., & Kim, S.-H. (1978) *J. Mol. Biol. 123*, 631–660.
Hore, P. J. (1983) *J. Magn. Reson, 55*, 283–300.
Hyde, E. I., & Reid, B. R. (1985) *Biochemistry 24*, 4307–4314.
Jack, A., Ladner, J. E., Rhodes, D., Brown, R. S., & Klug, A. (1977) *J. Mol. Biol. 111*, 315–328.
Kahn, A. S., & Roe, B. A. (1988) *Science 241*, 74–79.
Kohwi, Y., & Kohwi-Shigamatsu, T. (1988) *Proc. Natl. Acad. Sci. U.S.A. 85*, 3781–3785.
Kopper, R., Schmidt, P. G., & Agris, P. F. (1983) *Biochemistry 22*, 1396–1401.
Labuda, D., & Porschke, D. (1982) *Biochemistry 21*, 49–53.
Moras, D., Comarmond, M. B., Fischer, J., Weiss, R., & Thierry, J. C. (1980) *Nature 288*, 669–674.
Orbons, L. P. M., van der Marel, G. A., van Boom, J. H., & Altona, C. (1986) *Nucleic Acids Res. 14*, 4187–4196.
Orbons, L. P. M., van der Marel, G. A., van Boom, J. H., & Altona, C. (1987) *J. Biomol. Struct. Dyn. 4*, 939–963.
Otting, G., Grutter, R., Leupin, W., Minganti, C., Gamesh, K. N., Sproat, B. S., Gait, M. J., & Wuthrich, K. (1987) *Eur. J. Biochem. 166*, 215–220.
Pequette, J., Nicoghosian, K., Qi, G., Beauchemin, N., & Cedergren, R. (1990) *Eur. J. Biochem. 189*, 259–265.
Pilch, D. S., Levenson, C., & Shafer, R. H. (1990) *Proc. Natl. Acad. Sci. U.S.A. 87*, 1942–1946.
Pinnavaia, T. J., Miles, H. T., & Becker, E. D. (1975) *J. Am. Chem. Soc. 97*, 7198–7200.
Puglisi, J. D., Wyatt, J. R., & Tinoco, I., Jr. (1990) *Biochemistry 29*, 4215–4226.
Quigley, G. J., Teeter, M. M., & Rich, A. (1978) *Proc. Natl. Acad. Sci. U.S.A. 75*, 64–68.
Reid, B. R. (1981) *Annu. Rev. Biochem. 50*, 969.
Roy, S., Weinstein, S., Borah, B., Nickol, J., Appella, E., Sussman, J. L., Miller, M., Shindo, H., & Cohen, J. S. (1986) *Biochemistry 25*, 7417–7423.
Saenger, W. (1984) *Principles of Nucleic Acid Structure*, Springer-Verlag, New York.
Schimmel, P. (1989) *Biochemistry 28*, 2747–2759.
Schmidt, P. G., Sierzputowska-Gracz, H., & Agris, P. F. (1987) *Biochemistry 26*, 8529–8534.
Sinha, N. D., Biernat, J., McManus, J., & Koster, H. (1984) *Nucleic Acids Res. 12*, 4539–4557.
Smith, C., Schmidt, P. G., Petsch, J., & Agris, P. F. (1985) *Biochemistry 24*, 1434–1440.
Söll, D. (1990) *Experientia 46*, 1089–1096.
Striker, G., Labuda, D., & Vega-Martin, M. C. (1989) *J. Biomol. Struct. Dyn. 7*, 235–255.
Varani, G., Wimberly, B., & Tinoco, I., Jr. (1989) *Biochemistry 28*, 7760–7772.
Varani, G., Cheong, C., & Tinoco, I., Jr. (1991) *Biochemistry 30*, 3280–3289.
Werntges, H. (1985) Ph.D. Dissertation, University of Dusseldorf.
Williamson, J. R., & Boxer, S. G. (1989) *Biochemistry 28*, 2836–2843.
Wolk, S. K., Hardin, C. C., Germann, M. W., van de Sande, J. H., & Tinoco, I., Jr. (1988) *Biochemistry 27*, 6960–6967.
Woo, N. H., Roe, B. A., & Rich, A. (1980) *Nature 286*, 346–351.
Woodson, S. A., & Crothers, D. M. (1988) *Biochemistry 27*, 3130–3141.
Wyatt, J. R., Puglisi, J. D., & Tinoco, I., Jr. (1989) *Bioessays 11*, 100–106.
Wyatt, J. R., Puglisi, J. D., & Tinoco, I., Jr. (1990) *J. Mol. Biol. 214*, 455–470.
Yang, J.-H., Perreault, J.-P., Labuda, D., Usman, N., & Cedergren, R. (1991) *Biochemistry 29*, 11156–11160.